Applied and Environmental Microbiology

Antimicrobial Chemotherapy | Full-Length Text

Development of a luciferase-based Gram-positive bacterial reporter system for the characterization of antimicrobial agents

Nga Man Lam,[1] Tsz Fung Tsang,[1] Jiayi Qu,[1] Man Wai Tsang,[1] Yuan Tao,[1] Cheuk Hei Kan,[1] Qingyu Zou,[1] King Hong Chan,[2] Adrian Jun Chu,[1] Cong Ma,[2] Xiao Yang[1]

AUTHOR AFFILIATIONS See affiliation list on p. 17.

ABSTRACT Mechanistic investigations are of paramount importance in elucidating the modes of action of antibiotics and facilitating the discovery of novel drugs. We reported a luciferase-based reporter system using bacterial cells to unveil mechanisms of antimicrobials targeting transcription and translation. The reporter gene *Nluc* encoding NanoLuciferase (NanoLuc) was integrated into the genome of the Gram-positive model organism, *Bacillus subtilis*, to generate a reporter strain BS2019. Cellular transcription and translation levels were assessed by quantifying the amount of *Nluc* mRNA as well as the luminescence catalyzed by the enzyme NanoLuc. We validated this system using three known inhibitors of transcription (rifampicin), translation (chloramphenicol), and cell wall synthesis (ampicillin). The *B. subtilis* reporter strain BS2019 successfully revealed a decline in *Nluc* expression by rifampicin and NanoLuc enzyme activity by chloramphenicol, while ampicillin produced no observable effect. The assay was employed to characterize a previously discovered bacterial transcription inhibitor, CUHK242, with known antimicrobial activity against drug-resistant *Staphylococcus aureus*. Production of *Nluc* mRNA in our reporter BS2019 was suppressed in the presence of CUHK242, demonstrating the usefulness of the construct, which provides a simple way to study the mechanism of potential antibiotic candidates at early stages of drug discovery. The reporter system can also be modified by adopting different promoters and reporter genes to extend its scope of contribution to other fields of work.

IMPORTANCE Discovering new classes of antibiotics is desperately needed to combat the emergence of multidrug-resistant pathogens. To facilitate the drug discovery process, a simple cell-based assay for mechanistic studies is essential to characterize antimicrobial candidates. In this work, we developed a luciferase-based reporter system to quantify the transcriptional and translational effects of potential compounds and validated our system using two currently marketed drugs. Reporter strains generated in this study provide readily available means for identifying bacterial transcription inhibitors as prospective novel antibacterials. We also provided a series of plasmids for characterizing promoters under various conditions such as stress.

KEYWORDS reporter assay, antimicrobial agents, transcription inhibitors, translation inhibitors, antimicrobial resistance, drug discovery, novel antibiotics

Antimicrobial resistance (AMR) is a worldwide public health crisis with an estimated 4.95 million AMR-associated deaths globally in 2019 (1). Methicillin-resistant *Staphylococcus aureus* (MRSA) are leading pathogens for deaths attributable to AMR. While vancomycin, a bacterial cell wall synthesis inhibitor, is one of the first-line treatments for MRSA infections, strains of vancomycin-resistant *S. aureus* (VRSA) have already emerged (2–5). Continuous development of antimicrobial agents with novel modes of action is, therefore, vital to addressing the ongoing Antibiotic Crisis.

Editor Christopher A. Elkins, Centers for Disease Control and Prevention, Atlanta, Georgia, USA

Address correspondence to Xiao Yang, xiaoyang@cuhk.edu.hk, or Cong Ma, cong.ma@polyu.edu.hk.

Cong Ma and Xiao Yang contributed equally to this article.

The authors declare no conflict of interest.

See the funding table on p. 17.

Received 21 April 2024
Accepted 24 June 2024
Published 17 July 2024

Bacterial transcription and translation serve as valid targets for new drug discovery (6, 7). There are currently two classes of antibiotics (rifampicin and fidaxomicin) inhibiting bacterial RNA synthesis and several families of antibacterials acting on the translation machinery, including chloramphenicol, tetracyclines, and the macrolide family (such as erythromycin). While translation involves mainly ribosomes and translation factors (8, 9), bacterial transcription is carried out by RNA polymerase (RNAP) through interactions with various transcription factors. For example, an initiation factor σ must associate with bacterial RNAP to recognize a specific promoter. The primary initiation factor, σ^{70} in *Escherichia coli* and σ^{A} in *Bacillus subtilis*, governs expressions of housekeeping genes and plays a crucial role in cell viability (10, 11). These essential protein-protein interactions (PPIs), thus, present a wide host of potentially druggable targets for the discovery of antimicrobial agents (12–15).

Mechanistic investigations are key to elucidating the antimicrobial potency of antibiotics and to characterizing new drug candidates. Since bacterial RNA and protein synthesis are tightly regulated by various physiological factors, such as pH and temperature, monitoring these processes within cells can provide more insight into the mechanisms when combined with *in vitro* assays (16). A reporter gene such as *gfp* or *lacZ* (encoding for β-galactosidase) is usually inserted downstream of a specific promoter or fused with target genes (17–22). For example, a fluorescent protein-based system was established to monitor the SOS response and Shiga toxin production in enterohemorrhagic *E. coli* treated with transcription and translation inhibitors (17). Nevertheless, the low photostability of fluorescent proteins may hinder the result interpretation (23). Additionally, at low expression levels, GFP may be hampered by background noise, resulting in a low assay signal-to-noise ratio (24). Compared to fluorescent proteins, luciferase offers higher stability and sensitivity. NanoLuciferase (NanoLuc) is a small luciferase (19 kDa) engineered from the original deep-sea shrimp *Oplophorus gracilirostris* enzyme, exhibiting vigorous signal intensity and relatively high protein stability (25). NanoLuc has been applied in the screening of PPI inhibitors *in vitro*, measurement of PPI strength in living cells, as well as monitoring of tumor development in animal models (26–29). Despite the high intracellular stability of NanoLuc, most studies involving bacterial reporter strains only made use of the firefly-derived luciferase enzyme and were conducted in *B. subtilis* and *E. coli* (30–32).

Using NanoLuc as the reporter, we developed a bacterial cell-based system to evaluate the transcription and translation levels in the presence of antimicrobial agents. As the 3,000 bp length of the *lacZ* gene in recombinant *E. coli* allowed for the quantitative measurement of the transcription and translation elongation rate, we, therefore, offered *lacZ* as an alternative reporter in our system (33, 34). In this study, we constructed a suite of plasmids for the replacement of different promoters and reporter genes, followed by the generation of the *B. subtilis* reporter strain for use in cell-based assays.

The result was BS2019, where the reporter gene *Nluc* under the control of a xylose-inducible promoter was inserted into the genome of *B. subtilis*. The system was first validated using three marketed antibiotics with diverse but well-characterized modes of action, namely, rifampicin, chloramphenicol, and ampicillin (35, 36). Our system was further applied to examine the mechanisms of a previously discovered transcription inhibitor CUHK242 (published as Compound 54), which targeted the RNAP-σ interaction and demonstrated potent antimicrobial activity against a panel of Gram-positive pathogens (37).

RESULTS

Construction of the reporter plasmid system and the *B. subtilis* reporter strain BS2019

In this work, the recombinant plasmids were derived from the parent vector pSG1729 (Table 1; Fig. 1A), which integrated the promoter-reporter fragment into the *B. subtilis amyE* locus *via* double crossover (Fig. S1) (38). The initial reporter plasmid pCU314 was constructed by replacing the *gfp* gene with *Nluc*, driven by the xylose-inducible

TABLE 1 Plasmids used and constructed in this study

Plasmid	Genotype[a]	Source/construction
pSG1729	*bla amyE3' spc Pxyl-gfp mut1' amyE5'*	(38)
pET51b(+)_S-Luc_CLIP	*bla Pφ10-Nluc*	(39)
pCU251	*bla Pφ10-sigA-LgBiT-6×His-Tφ*	(27)
pCU252	*bla Pφ10-SmBiT-CH-6×His-Tφ*	(27)
pCU314	*bla amyE3' spc Pxyl-Nluc amyE5'*	This work. Reporter gene *Nluc* cloned in *Acc65*I and *Eco*RI cut pSG1729.
pCU344	*bla amyE3' spc* MCS *amyE5′*	This work. The fragment of spectinomycin and unitary restriction sites cloned in *Xba*I and *Eco*RV cut pCU314.
pCU354	*bla amyE3′ spc Nluc amyE5'*	This work. Reporter gene *Nluc* cloned in *Acc65*I and *Eco*RI cut pCU344.
pCU483	*bla amyE3' spc Pxyl-lacZ amyE5'*	This work. Reporter gene *lacZ* cloned in *Acc65*I and *Eco*RI cut pSG1729.

[a]*bla*, ampicillin resistance gene; *Pφ10*, phage T7 promoter; *spc*, spectinomycin resistance gene.

promoter (Table 1; Fig. 1B). pCU314 was transformed into the wild-type *B. subtilis* 168 (BS168) to generate the reporter strain BS2019 (Table 2). To offer an alternative to the reporter, we also substituted the *gfp* fragment with the *lacZ* gene. The resulting vector was named pCU483 (Table 1; Fig. 1C).

We further modified pCU314 to increase the versatility of the plasmid system. The region flanked by the *amyE5′* and *amyE3′* sequences was replaced by a fragment comprising the spectinomycin resistance gene *spc* and a new multiple cloning site (MCS) for the insertion of different promoters and reporter genes. The resulting vector was named pCU344 (Table 1; Fig. 1D). We then cloned the gene *Nluc* into pCU344 to obtain pCU354 (Table 1; Fig. 1E). pCU354 can be used to examine the use of various promoters by the *Nluc*-based reporter assay.

Validation and application of the reporter assay system

Throughout this study, we made extensive use of the newly generated *B. subtilis* reporter strain BS2019 for both system validation and subsequent mechanistic investigations. As the expression of an exogenous gene may impact bacterial growth following chromosome incorporation (40), we measured the growth rates of both BS2019 and wild-type BS168. The growth rates of non-induced BS2019 and BS168 were found to be comparable as shown in Fig. 2A. The doubling times of BS168 (47 min) and BS2019 without xylose induction (38 min) were slightly different, indicating that the gene insertion may affect bacterial growth to some extent. BS2019 treated with 1% xylose to induce *Nluc* gene expression saw no marked changes in its doubling time (Fig. 2A), suggesting that the expression of *Nluc* did not impact bacterial growth.

To evaluate the expression of the inducible reporter gene, *Nluc* mRNA transcript and the chemiluminescence resulting from NanoLuc activity were quantified. Following the addition of 1% xylose, a twofold increase in BS2019 *Nluc* mRNA level was detected within 5 min, whereas the control group showed no significant changes (Fig. 2B). Similarly, the

TABLE 2 Strains used and constructed in this study

Strain	Genotype[a]	Source/construction
B. subtilis 168	*trpC2*	
BS2019	*trpC2 ΩamyE::pCU314(spc Pxyl–Nluc)*	This work. *B. subtilis* 168 transformed with pCU314.

[a]Ω, insertion; *spc,* spectinomycin resistance gene.

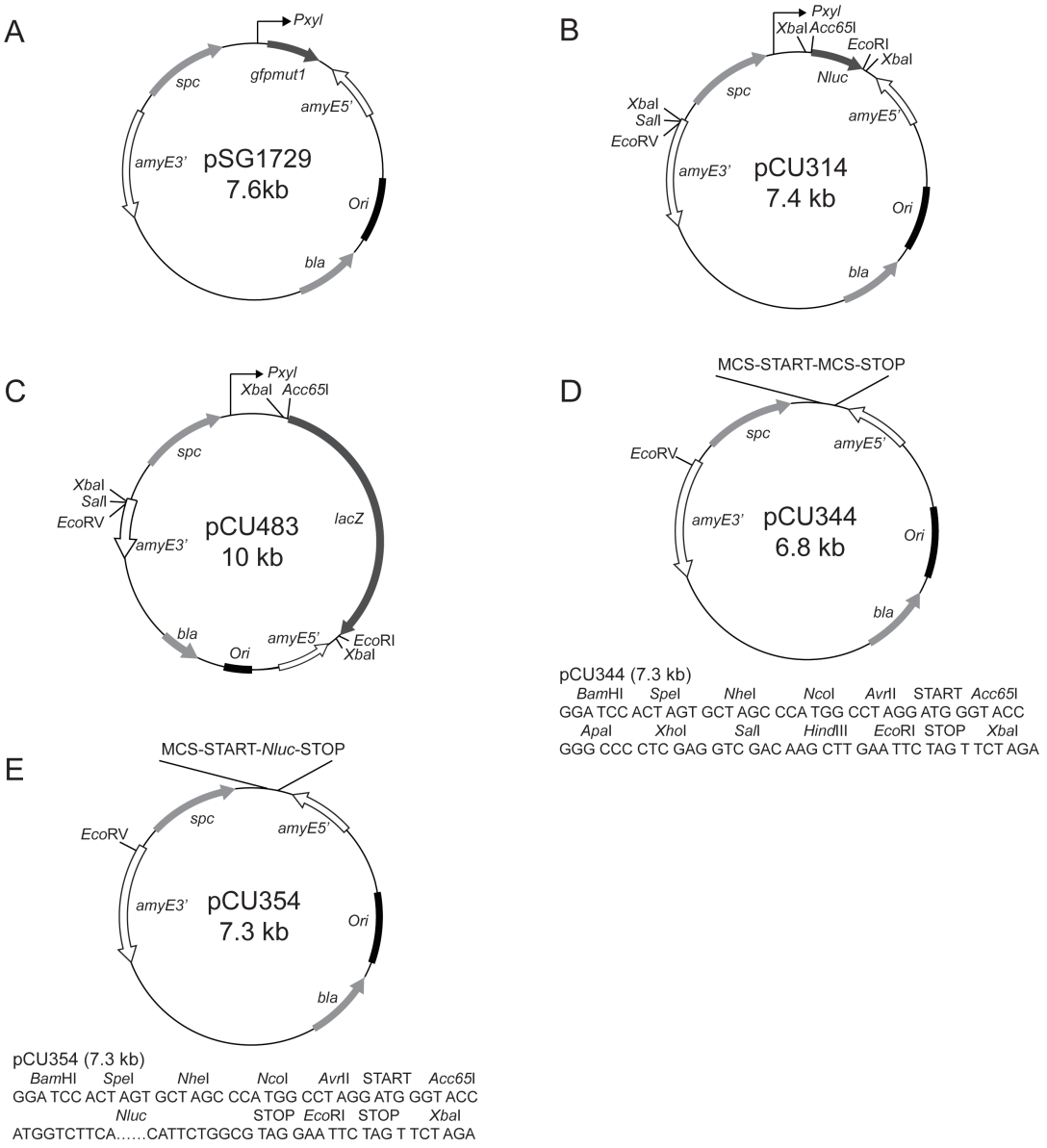

FIG 1 Plasmids for reporter strain construction. (A) The parent vector pSG1729.(38) (B) pCU314 encoding the *Nluc* gene under the control of *PxyI*. (C) pCU483 encoding *lacZ* driven by *PxyI*. (D) pCU344 with the promoter and reporter gene fragment replaced by multiple cloning site (MCS). (E) pCU354 encoding *Nluc* upstream the start codon for promoter replacement. *PxyI*, xylose-inducible promoter; *spc*, spectinomycin resistance gene; *bla*, ampicillin resistance gene; *Ori*, plasmid replication origin; MCS, multiple cloning site.

luminescence signal generated by NanoLuc saw a steady 20% rise within 5 min, while that of the non-induced group remained relatively constant. The results suggested that *Nluc* gene expression can be induced by the addition of xylose and became readily detectable within the experimental interval of 5 min for the reporter assay.

We validated the reporter assay using three widely used antibacterials, rifampicin, chloramphenicol, and ampicillin, which target bacterial transcription, translation, and cell wall synthesis, respectively (41–45). To minimize the effects of potential antibiotic-induced stress response, the drug concentrations used in the assay should be relative to their antimicrobial activity as baselines, represented by their respective minimum inhibitory concentrations (MICs). MIC was defined as the lowest concentration of antimicrobial agent without eliciting visible bacterial growth, where its value was obtained by performing broth microdilution as stipulated in guidelines from the

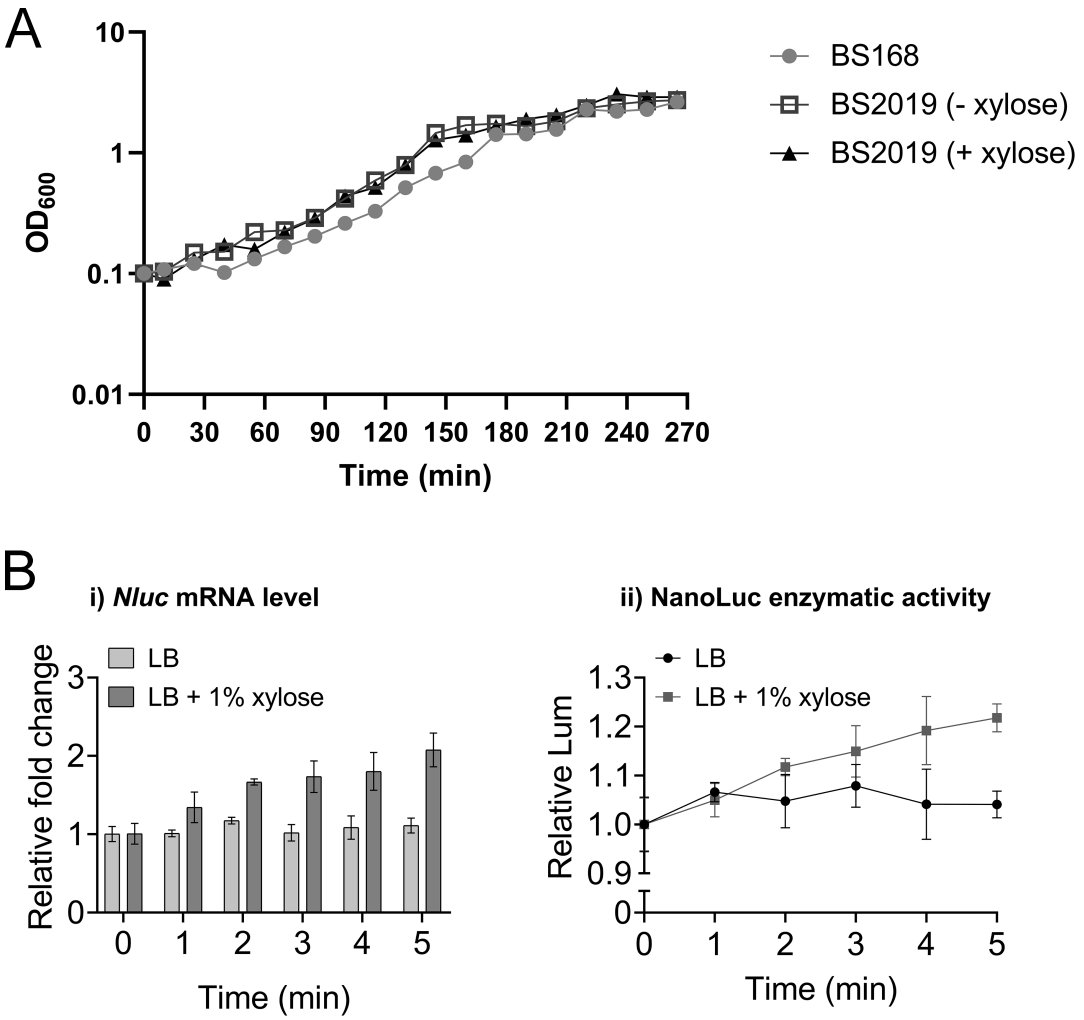

FIG 2 Effects of 1% xylose supplementation on (A) growth and (B) *Nluc* expression of BS2019. Relative fold change of (i) *Nluc* mRNA level and (ii) relative luminescence intensity generated by NanoLuc were presented as mean ± SD. Lum, luminescence intensity.

Clinical and Laboratory Standards Institute (CLSI) (46). As shown in Table 3, rifampicin, chloramphenicol, and ampicillin all demonstrated diverse MIC values against BS2019. Notably, CUHK242 also indicated good antimicrobial activity. The varying MICs exhibited by these compounds against BS2019 highlighted the importance of taking their distinct antimicrobial mechanisms of action into consideration in subsequent experiments.

Time-kill kinetics assay was performed to characterize the bactericidal activity of the three antibacterial drugs alongside CUHK242 at their ½ ×, 1 ×, and 4 × MICs against BS2019 (Fig. 3). Even at sub-MIC levels, both rifampicin and CUHK242 resulted in the eradication of viable BS2019 colonies below detection limit within 4 h (Fig. 3A and D), while ampicillin at all doses displayed strong bactericidal effect in half the time span (Fig. 3C). On the other hand, chloramphenicol remained mostly bacteriostatic against BS2019 (Fig. 3B).

TABLE 3 Antimicrobial activity of antimicrobial agents against BS2019

	Rif[a]	Chl[b]	Amp[c]	CUHK242
MIC (μg/mL)	0.125	8	0.125	2

[a]Rif, rifampicin.
[b]Chl, chloramphenicol.
[c]Amp, ampicillin.

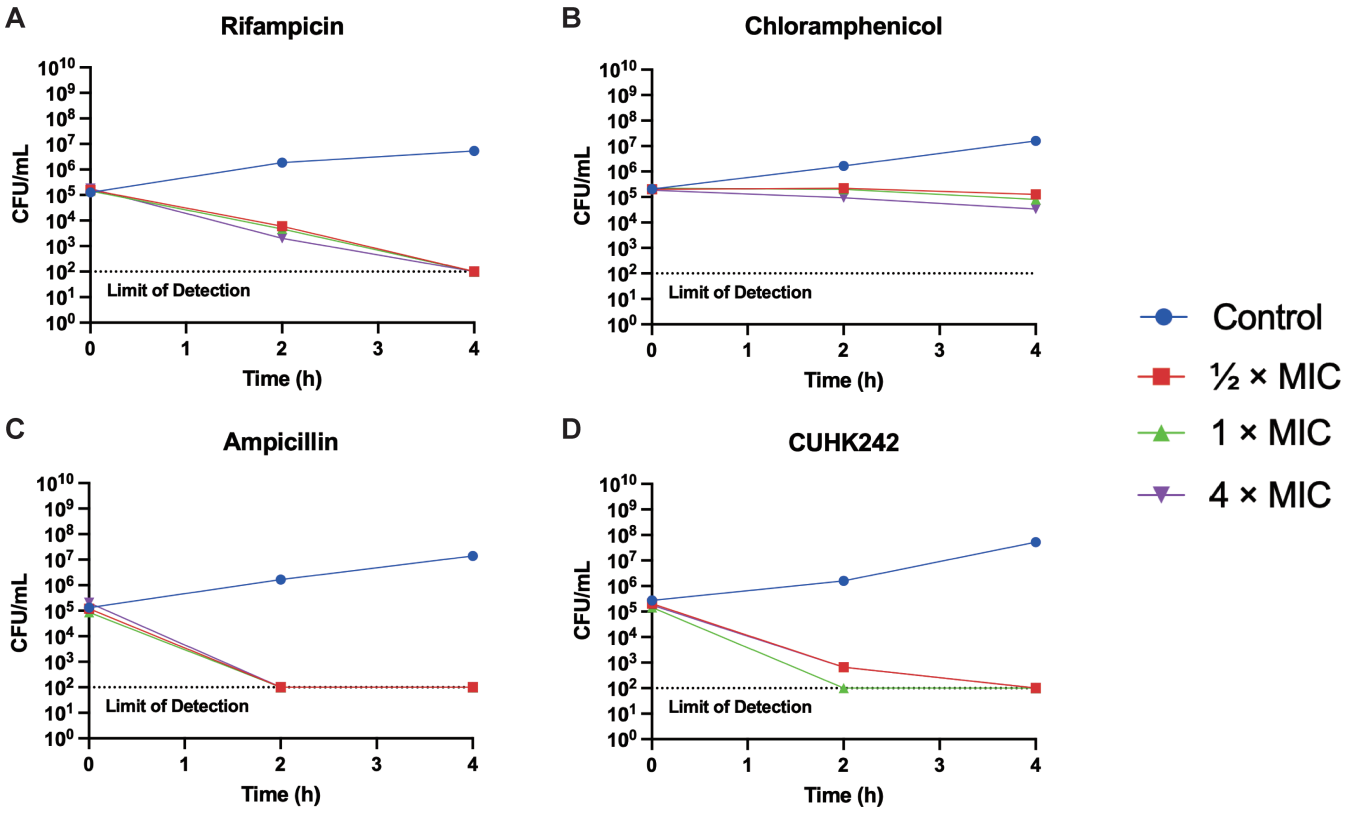

FIG 3 Effects of (A) rifampicin, (B) chloramphenicol, (C) ampicillin, and (D) CUHK242 on the time-kill kinetics of BS2019. The samples were harvested at 0, 2, and 4 h.

We surmised that ½ × MIC may serve as a sublethal concentration mutual to the antimicrobial agents used which could reflect a sufficiently growth-inhibiting phenotype with minimum stress response in biological investigations involving BS2019 (47). The time-kill kinetics of all test compounds over the reporter assay duration (5 min) were assessed. Chloramphenicol, ampicillin, and rifampicin, at their respective ½ × MICs, all showed negligible stress on BS2019 growth, while CUHK242 greatly decreased viable colony count of BS2019 by >10-fold at ½ × but not ¼ × MIC (Fig. S2). To alleviate potential lethal effects, the lower dose ¼ × MIC of CUHK242 was consequently included in experimental setups for comparison where appropriate.

To examine *Nluc* gene expression under different treatments, BS2019 was grown to exponential phase prior to the addition of 1% xylose and the selected antimicrobial agents at ½ × MIC. Cellular total RNA was extracted for the detection of *Nluc* transcripts by RT-qPCR, whereas the cell lysates were subjected to enzymatic assay probing for the luminescence reaction catalyzed by NanoLuc. Compared to the untreated group, rifampicin treatment decreased the relative *Nluc* expression level by around twofold and a general reduction in detected luminescence signal (Fig. 4A). The untreated group, on the other hand, saw a 20% increase in enzymatic activity over the course of the assay (Fig. 4A). While chloramphenicol did not affect *Nluc* mRNA synthesis, a significant decline in luminescence signal was detected, suggesting a greatly impaired NanoLuc production rate in line with its mechanism of action (Fig. 4B). Ampicillin, as a cell wall synthesis inhibitor, appeared to have disrupted neither *Nluc* expression nor luminescence levels, which was in line with its drug mechanism and did not impact bacterial transcription and translation (Fig. 4C). Overall, the characteristically divergent effects of antibiotics with known mechanisms of action were clearly recognizable using our reporter system, which strongly supported the feasibility of utilizing the proposed assay for the assessment of transcription- and translation-inhibiting antibacterial agents.

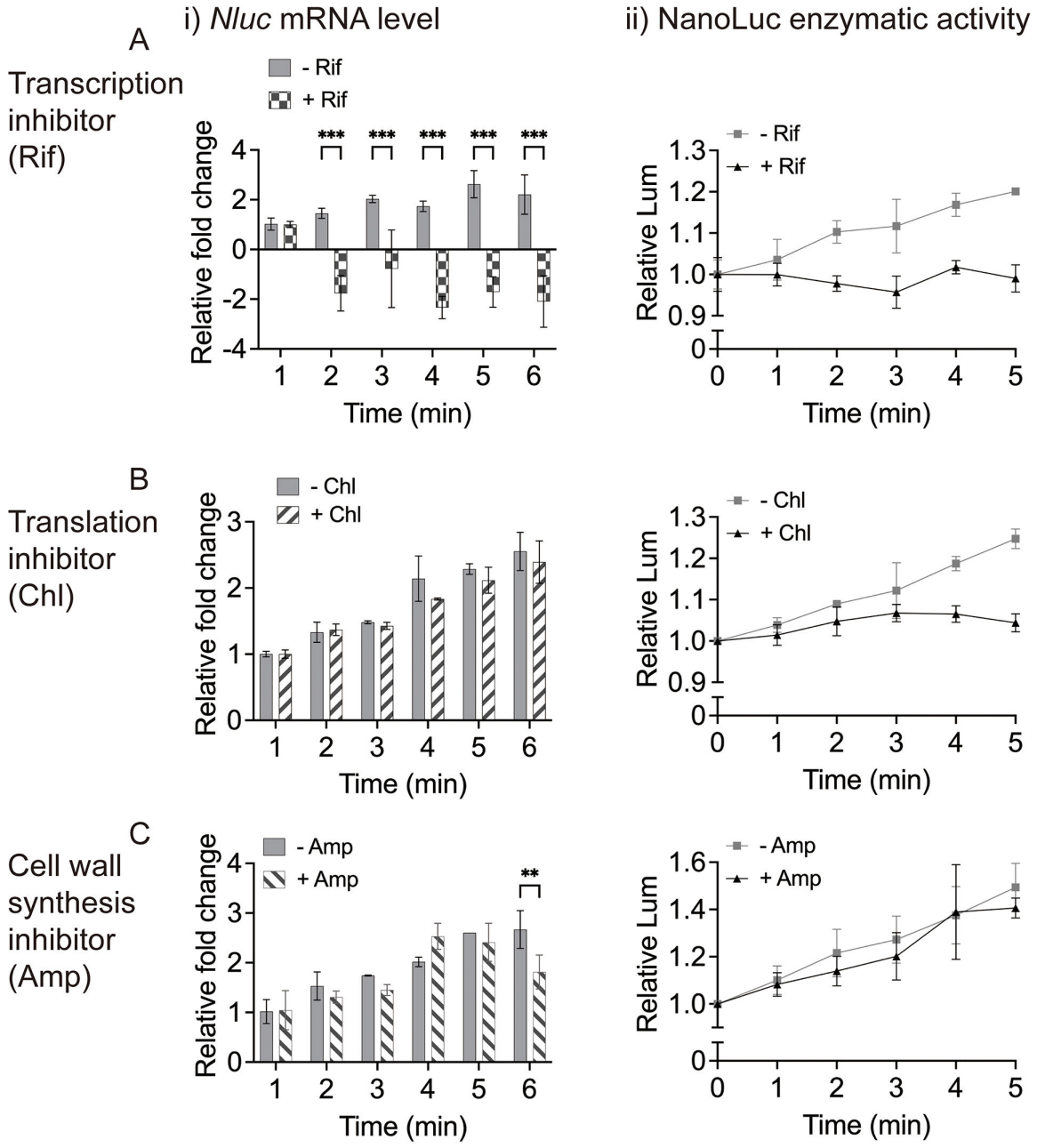

FIG 4 The effects of rifampicin, chloramphenicol, and ampicillin on *Nluc* expression in the reporter strain developed in this study (BS2019). (A) Expression of *Nluc* under treatment with ½ × MIC rifampicin (Rif). (B) Expression of *Nluc* under treatment with ½ × MIC chloramphenicol (Chl). (C) Expression of *Nluc* under treatment with ½ × MIC ampicillin (Amp). (i) Relative fold change of *Nluc* mRNA level and (ii) relative luminescence intensity generated by NanoLuc were presented as mean ± SD. lum, luminescence intensity. Technical repeats were performed for data reproducibility.

Using the validated cell-based assay, we proceeded to characterize CUHK242, which was designed to interrupt the initiation step in RNA synthesis. As prior *in vitro* studies already demonstrated transcription inhibition exerted by CUHK242 (published as Compound 54) (37), in this study, our aim was to investigate its impact on transcription within cells. Upon treating BS2019 with CUHK242 at ½ × MIC, a substantial suppression in both *Nluc* mRNA and luminescence signal was noted in comparison to the untreated control group (Fig. 5A). This reduction in cellular *Nluc* mRNA possibly resulted in diminished NanoLuc synthesis and, thus, may have contributed to a proportionally

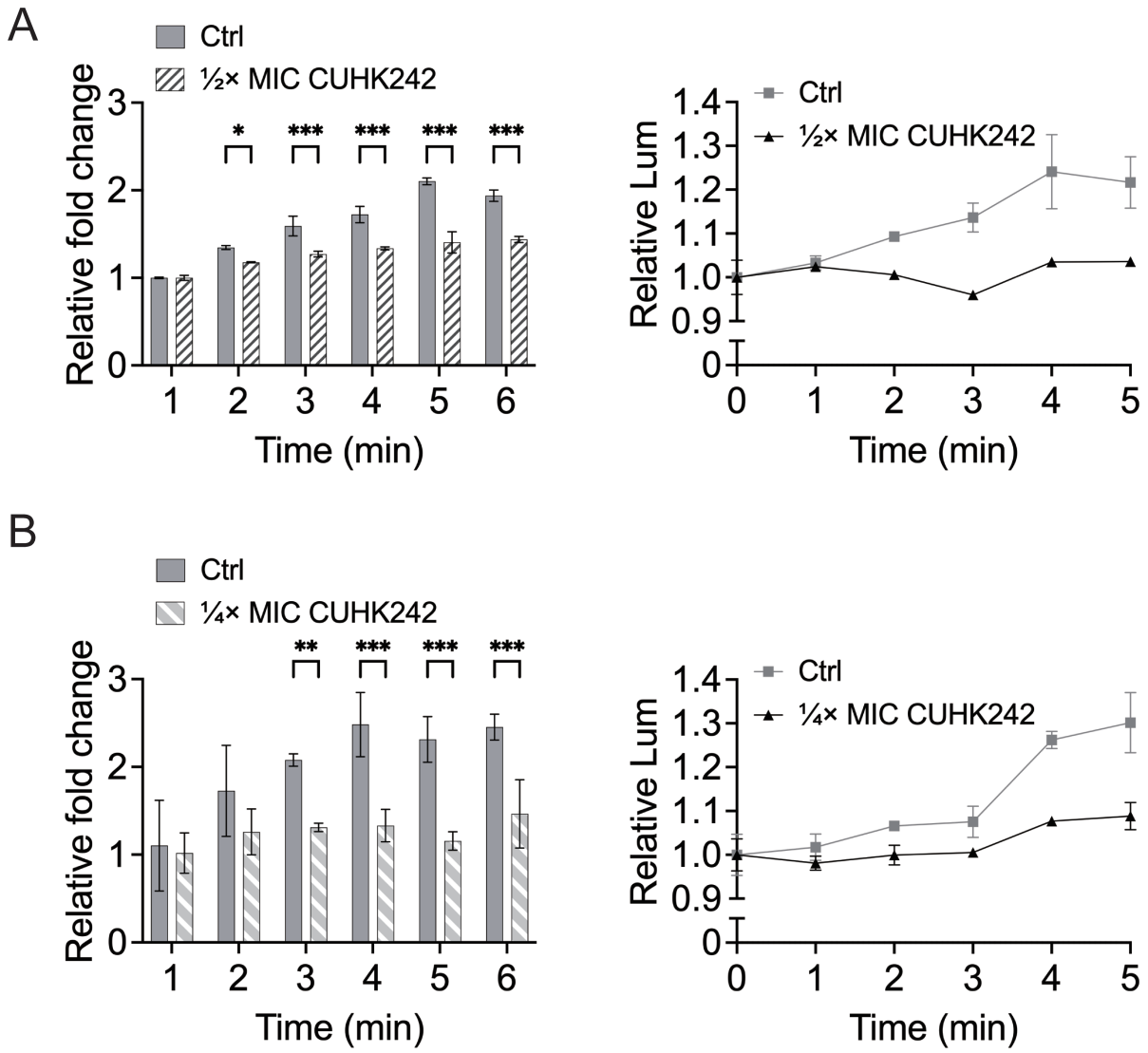

FIG 5 Effect of CUHK242 on *Nluc* expression by BS2019. (A) Relative fold change of *Nluc* mRNA and (B) relative luminescence intensity generated by NanoLuc were presented as mean ± SD. Lum, luminescence intensity. Technical repeats were performed to ensure data reproducibility.

diminished luciferase activity. At ¼ × MIC CUHK242, both *Nluc* expression level and NanoLuc activity showed a modest reduction compared to the control group (Fig. 5B).

Antimicrobial activity of CUHK242 against MRSA and VRSA

We tested CUHK242 against a panel of MRSA and VRSA strains representing clinically significant lineages, as well as laboratory-generated strains representing various resistance mechanisms. The MRSA strains include hospital-associated MRSA (HA-MRSA) sequence type (ST) 239, the dominant strain in East, Southeast, and South Asia; ATCC BAA-43, a Brazilian clone; ATCC BAA-44, an Iberian clone; HA-MRSA ST45, which was increasingly prevalent among MRSA bloodstream isolates from 1999 to 2005 in Hong Kong; community-associated MRSA (CA-MRSA) ST30 and ST59, both prevalent clones in Hong Kong and other Asian countries; CA-MRSA USA300 JE2 LAC, a CA-MRSA strain epidemic in the United States; CA-MRSA ST22 which is widespread across Europe; SA-1199B, a fluoroquinolone-resistant laboratory-derived strain; SA-RN4220-pUL5054, a macrolide-resistant lab strain; SA-APH2″-AAC6′, a gentamicin-resistant lab strain; SA-ANT4′, a fusidic acid-resistant lab strain (48–54). According to CLSI guidelines, drug

resistance was defined as MIC values greater than the clinical breakpoints (≥16 µg/mL for vancomycin and gentamicin, and ≥4 µg/mL for oxacillin, ciprofloxacin, and rifampicin against *S. aureus*) (46). The tested MRSA species saw concomitant resistance to multiple antibiotics, such as oxacillin, gentamicin, and kanamycin, while all were susceptible to CUHK242 with stable MIC values ranging between 2 and 4 µg/mL, comparable to the first-line drug vancomycin (Table 4).

The VRSA strains tested in this work were provided by the Network on AMR in *S. aureus* (NARSA) for distribution by BEI Resources, NIAID, NIH, and administrated by ATCC (Manassas, Virginia, United States). These included VRSA-1 (NR-46410/*S. aureus* strain HIP11714), VRSA-2 (NR-46411/*S. aureus* strain HIP11983), VRSA-3a (NR-46412/*S. aureus* strain HIP13170) and VRSA-3b (NR-46413/*S. aureus* strain HIP13419), VRSA-4 (NR-46414/*S. aureus* strain HIP14300), VRSA-5 (NR-46415/*S. aureus* strain HIP15178), VRSA-7 (NR-46417/*S. aureus* strain AIS 2006045), VRSA-8 (NR-46418/*S. aureus* strain 71080), VRSA-9 (NR-46419/*S. aureus* strain AIS 080003), VRSA-10 (NR-46420/*S. aureus* strain AIS 1000505), and VRSA-11a (NR-46421/*S. aureus* strain AIS 1001095). Most VRSA strains used were USA100 isolates except for VRSA-3a and VRSA-2b, which were USA800 isolates. USA100 strains are the most common pulse-field type of VRSA from nasal cultures in the United States, followed by USA800 (55, 56). As shown in Table 5, CUHK242 demonstrated outstanding antimicrobial activities with MICs of 2–4 µg/mL against all tested VRSA strains. In contrast, most strains were desensitized to the bacterial cell wall synthesis inhibitors vancomycin and oxacillin, the translation inhibitors gentamicin and kanamycin, as well as the DNA gyrase inhibitor ciprofloxacin. Our compound CUHK242 demonstrated remarkable anti-staphylococcal properties and has promising prospect as a new treatment option for highly drug-resistant staphylococcal infections.

CUHK242 inhibits RNAP-σ interaction *in vitro*, kills MRSA without resistance selection, and attenuates secretion of MRSA hemolytic toxin

The PPI inhibitory activity of compound CUHK242 was evaluated using an in-house developed luciferase complementation assay (27). In this assay, a specific PPI of two proteins carrying the complementary NanoLuc fragment tags contributed to the NanoLuc reformation. Luminescence signals that arose from the reconstituted NanoLuc activity were probed to assess PPI, while a decrease in chemiluminescence resulted from PPI inhibitors. In this work, the RNAP clamp helix (CH) fragment and σ factor were

TABLE 4 Antimicrobial activity of CUHK242 against *S. aureus* type strains (ATCC 25923 and 29213), representative MRSA and lab-derived drug-resistant strains, presented as MICs (µg/mL)

	CUHK242	Van[a]	Oxa[b]	Gen[c]	Cip[d]	Rif[e]	Kan[f]
ATCC 25923	2	2	0.5	0.5	1	0.0156	2
ATCC 29213	2	1	0.5	2	1	0.0078	16
HA-MRSA ST239	2	1	256	>64	32	0.0039	>64
ATCC BAA43	2	1	>256	>64	32	>2	>64
ATCC BAA44	2	1	256	>64	32	2	>64
HA-MRSA ST45	4	1	2	32	16	0.0078	>64
CA-MRSA ST30	2	1	4	1	1	0.0078	4
CA-MRSA ST59	2	1	2	0.5	1	0.0078	>64
CA-MRSA USA300	2	1	8	2	16	0.0078	8
CA-MRSA ST22	2	1	32	1	>64	0.0078	2
SA-1199B	2	1	≤0.25	1	16	0.0078	2
SA-RN4220-pUL5054	2	1	≤0.25	0.5	0.5	0.0078	2
SA-APH2″-AAC6′	2	1	128	>64	16	2	>64
SA-ANT4′	2	1	4	>64	16	0.0078	>64

[a]Van, vancomycin.
[b]Oxa, oxacillin.
[c]Gen, gentamicin.
[d]Cip, ciprofloxacin.
[e]Rif, rifampicin.
[f]Kan, kanamycin.

TABLE 5 Antimicrobial activity of CUHK242 against representative VRSA strains, presented as MICs (μg/mL)

	CUHK242	Van[a]	Oxa[b]	Gen[c]	Cip[d]	Rif[e]	Kan[f]
VRSA-1	4	>256	256	64	>64	>2	>64
VRSA-2	2	256	256	64	>64	≤0.002	>64
VRSA-3a	4	64	64	64	>64	0.0078	>64
VRSA-3b	4	256	128	>64	>64	0.0078	>64
VRSA-4	2	128	128	4	>64	0.0078	>64
VRSA-5	2	>256	32	>64	>64	0.0156	>64
VRSA-7	2	256	16	>64	>64	0.0078	>64
VRSA-8	2	>256	64	>64	>64	0.0039	>64
VRSA-9	4	>256	16	>64	>64	0.0078	>64
VRSA-10	2	>256	128	4	>64	0.0078	>64
VRSA-11a	2	>256	≤0.25	4	64	2	>64

[a]Van, vancomycin.
[b]Oxa, oxacillin.
[c]Gen, gentamicin.
[d]Cip, ciprofloxacin.
[e]Rif, rifampicin.
[f]Kan, kanamycin.

fused with the two NanoLuc tags, respectively. CUHK242 suppressed the luminescence emission in a dose-dependent manner with IC_{50} determined at 117.7 ± 5.91 μM (Fig. 6A).

The time- and dose-dependent relationship between the addition of CUHK242 at concentrations relative to its MIC and bacterial growth was determined for the MRSA USA300 strain JE2 LAC (obtained from BEI Resources). Growth of MRSA cells was shown to be inhibited following 4 h of incubation in the presence of the compound at levels equal to or above MIC (Fig. 6B). Overall, CUHK242 exhibited a largely bacteriostatic profile against a clinically significant drug-resistant *S. aureus* strain, with only modest and gradual decreases in CFU counts at higher concentrations at later time points.

To assess whether AMR would emerge under selective pressure, an *S. aureus* ATCC 29213 type strain and an MRSA USA300 strain JE2 LAC were continuously exposed to sub-inhibitory levels of either CUHK242 or rifampicin. Over the course of 15 days, rifampicin showed a gradual rise in daily recorded MIC values, amounting to an increase of more than 30,000-fold from its original MIC upon the experimental endpoint, whereas CUHK242 showed only minor fluctuations in MIC, within the fourfold threshold indicative of resistance emergence (Fig. 6C and D). This suggested that CUHK242 was less likely to select for resistant isolates compared to the RNA synthesis inhibitor class drug rifampicin, supporting its potential use in clinical scenarios where antibiotic resistance is frequent.

The effects of CUHK242 treatment at sub-inhibitory concentrations on mitigating damage to host RBCs (red blood cells) induced by the *S. aureus* secretory exotoxin α-toxin (α-hemolysin) was also assessed. Results showed that α-toxin levels found in compound-treated overnight cultures of USA300 strain JE2 LAC all required up to 64-fold dilution before their lytic effects on rabbit RBC were fully removed (Fig. 7). This suggested that, compared to both vancomycin- and rifampicin-treated groups, as well as untreated control groups, CUHK242 treatment was non-inferior in its ability to attenuate a major virulence factor of MRSA by protecting host erythrocytes from hemolysis *in vitro*.

DISCUSSION

Validation of the NanoLuc-based bacterial reporter system

System validation was undertaken by investigating *Nluc* gene expression over a span of 5 min following antibiotic treatment, as reporter gene showed measurable expression levels within the designated interval while any potential drug-induced stress responses can be minimized to prevent skewing. For example, chloramphenicol can trigger a stringent response that reduces GTP, potentially suppressing reporter gene transcription (57). Rifampicin can also stimulate the synthesis of the RNAP catalytic subunits β and β′

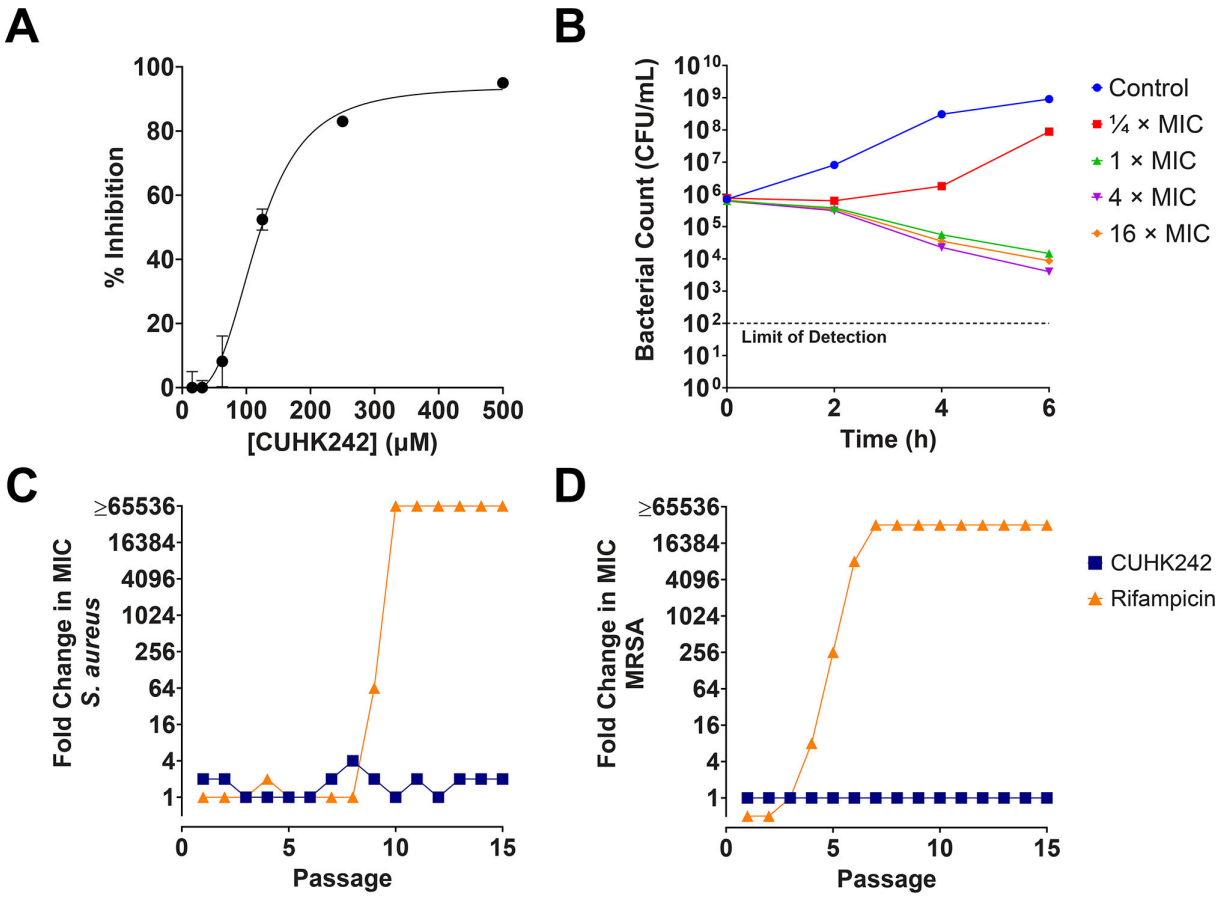

FIG 6 (A) Inhibitory curve of compound CUHK242 measured by luciferase complementation assay. Technical repeats were performed for data reproducibility. (B) Effects of increasing concentrations CUHK242 on the time-kill kinetics of MRSA USA300 strain JE2 LAC. Resistance development of (C) *S. aureus* ATCC 29213 and (D) MRSA USA300 strain JE2 LAC to CUHK242 (indigo squares) and rifampicin (orange triangles). Results were presented as fold changes (in $\log_2$) in MICs relative to their respective initially recorded values. Experiments were performed in triplicates, and representative data were shown.

after 20 min from administration, where this cellular response may lead to elevated *Nluc* transcription levels (58–60). In addition, ampicillin at high concentrations (100 µg/mL) can promote the expression of the transcription factor Spx which efficiently activates RNA synthesis in *B. subtilis* (61). Nonetheless, the impact of these drug-induced stress responses was not observed in our assay, which was conducted within the span of just 5 min.

Our findings were highly consistent with the well-characterized mechanisms of the tested drugs. Rifampicin is the canonical bacterial RNA synthesis inhibitor that blocks RNA extension (62). It can be inferred that the repression of *Nluc* transcription led to insufficient NanoLuc production, represented by the decline in the luminescence signal. Our data can reflect the translation-inhibiting effects exerted by chloramphenicol, which binds to the bacterial ribosome to prevent peptide bond formation (63, 64). Ampicillin is a β-lactam antibiotic that interacts with penicillin-binding proteins to inhibit peptidoglycan crosslinking, a key process in cell wall synthesis (35, 36). It is, therefore, reasonable that the cell wall inhibitor ultimately did not disturb both RNA and protein synthesis. Our reporter strain BS2019 was shown to respond differently in the presence of antibiotics with divergent drug targets, supporting its use in the identification of potential antibiotic candidates acting on bacterial transcription and translation.

Previous studies made use of *B. subtilis* strains producing recombinant GFP fused to essential transcription factors to examine the cellular effects of inhibitors, showing the delocalizing effects upon the bacterial transcription complexes (65, 66). In this work, we

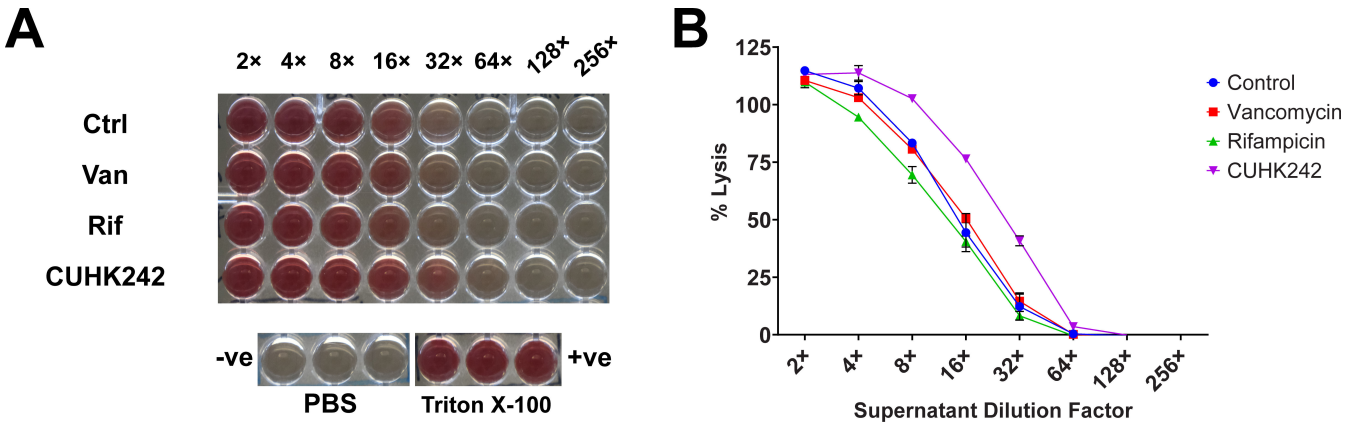

FIG 7 Effect of treatment at sub-inhibitory levels of CUHK242, vancomycin, and rifampicin on rabbit RBC lysis induced by α-toxin produced by MRSA USA300 strain JE2 LAC, compared to untreated control group. Results were shown as (A) photographic image of hemoglobin release and (B) % cell lysis at each twofold dilution series normalized against fully lysed RBCs treated with Triton X-100. Experiments were performed in triplicates and representative figures were shown. Van, vancomycin; Rif, rifampicin.

generated a *B. subtilis* reporter strain which synthesized NanoLuc for signal detection. Compared to the GFP fusion strains, our assay provides a more quantitative way to characterize RNA synthesis inhibitors. In addition to higher sensitivity that comes with luminescence-based assays, direct comparison between transcription inhibitors was also made possible due to distinct NanoLuc activity profiles under different treatments.

Cellular effects and antimicrobial activities of CUHK242

Through computational drug screening and design methods, we previously reported the antimicrobial compound CUHK242 which was designed to inhibit the essential interaction between bacterial RNAP and the initiation factor σ. Previous investigations demonstrated the antimicrobial effects against multiple Gram-positive pathogens and *in vitro* transcription inhibition by the compound. In this work, we applied the newly developed reporter system to examine CUHK242 mechanistically and further characterize its antimicrobial effects. Similar to rifampicin, CUHK242 suppressed both transcription and translation of the reporter gene *Nluc* at sublethal doses. The data suggested that CUHK242 can, indeed, inhibit RNA synthesis in cells, resulting in a simultaneous reduction in protein synthesis. These observations were in concordance with the designated role of CUHK242 as a bacterial transcription inhibitor. The role of CUHK242 as the RNAP-σ PPI inhibitor was consolidated by the *in vitro* PPI inhibition assay. From the *in vitro* and cell-based data, it can be extrapolated that the impaired RNA synthesis was correlated to the incomplete RNAP-σ interaction, which represented a critical step in transcription initiation. Results from time-kill kinetics assays revealed the bactericidal activity of CUHK242 against the Gram-positive model species *B. subtilis*. The investigation was also expanded for its activity against panels of clinical MRSA and VRSA lineages, as well as lab-derived resistant strains. All tested multi-drug-resistant *S. aureus* strains were susceptible to CUHK242, while most of them were resistant or showed desensitization toward multiple classes of antibiotics, including the first-line drugs vancomycin and oxacillin, as well as alternative chemotherapeutants such as gentamicin. Repeated passaging of both drug-susceptible and resistant strains of *S. aureus* did not give rise to CUHK242-resistant variants. While a time-kill assay painted a largely bacteriostatic picture for CUHK242 when directly administered against an MRSA USA300 strain, the compound was ultimately able to attenuate the effects of a major virulence factor α-toxin. Future investigations can focus on in-depth characterization such as binding site identification, evaluation of cytotoxicity in mammalian cell lines, and *in vivo* efficacy studies using animal infection models.

Further assay development

A major limitation was that only *B. subtilis* can be used for generating reporter strains due to the plasmid design, and therefore, the system may not be applicable in cases where *B. subtilis* is not susceptible to a treatment compound. Biological differences in the colonies used in each technical repeat could potentially contribute to inconsistencies in *Nluc* transcript and NanoLuc enzyme activity across different trials (67). Notwithstanding these discrepancies, they did not seem to impact the effects of the three antimicrobial agents evaluated during the assay validation stage. The system serendipitously demonstrated a basal expression of the *Nluc* gene, which is indicative of difficulties when attempting to detect minor changes. Promoters with tighter gene expression control, such as the arabinose-inducible promoter, could be employed to reduce basal gene expression and offset any potential effects (68).

Apart from facilitating drug discovery, the reporter assay may also serve as a valuable tool in other applications. For example, it can monitor the reporter gene expression under different environmental changes such as ethanol levels, osmotic pressure, and temperature, which altered transcription mediated by an alternative initiation factor σ^B in *B. subtilis* (69, 70). The promoters regulating stress-induced expression can be inserted upstream of the reporter genes such that their activities can also be investigated.

Conclusion

In summary, we developed a cell-based assay intended for characterizing transcription and translation inhibitors for novel antimicrobial discovery. To the best of our knowledge, our reporter assay is the first quantitative approach to evaluate transcription and translation activity using the *Nluc* reporter gene in the Gram-positive model organism *B. subtilis*. The system can be applied to achieve a better understanding of transcription and translation inhibition by antimicrobial agents. The reporter assay showed potential for application in the characterization and discovery of novel antimicrobial agents. This system also offers a suite of reporter plasmids that are systematically designed to facilitate the substitution of promoters and reporter genes of interest.

MATERIALS AND METHODS

Construction of plasmid vectors

E. coli strain DH5α was used for cloning in this study. Primers used for cloning are listed in Table S1. In brief, the *Nluc* reporter gene used in this study was amplified from pET51b(+)_S-Luc_CLIP by primer nlucF and nlucR. The amplicons were digested with *Acc65*I and *Eco*RI and inserted into similarly cut pSG1729 to construct pCU314. The *lacZ* reporter gene amplified from *E. coli* was digested with *Acc65*I and *Eco*RI and inserted into similarly cut pSG1729 to construct pCU483. To construct a vector with the spectinomycin resistance gene and unitary restriction sites, DNA fragments of the spectinomycin resistance gene with MCS (purchased from Thermo Fisher) were amplified by primers Fragments_F and Fragments_R. The amplicons were digested with *Eco*RV and *Xba*I and inserted into similarly cut pCU314 to construct pCU344. The reporter gene *Nluc* was then amplified from pCU314 by primers Nluc_Acc65I_F and Nluc_EcoRI_R. The amplicons of *Nluc* were cut with *Acc65*I and *Eco*RI and inserted into similarly cut pCU344 to construct pCU354.

Construction of reporter strains

The wild-type *B. subtilis* strain BS168 was used for reporter strain construction. The plasmid transformation approach for constructing reporter strains was adapted from the methods as described by Lewis and Marston (38). In brief, overnight cultures of *B. subtilis* in MM competence media (Table S2) were inoculated into 10 mL pre-warmed starvation media (Table S2) and incubated at 37 °C for 2 h. Ten microliters of pCU314

was mixed with 0.4 mL culture. Following the incubation at 37 °C for 1 h, 100 µL reaction mixture was plated onto the LB agar plate with 15 µg/mL spectinomycin for selection and incubated overnight at 37 °C. The resulting plates were stained with iodine solution to verify that the genome insertion took place at the *amyE* locus. NanoLuc assay was conducted to further confirm the validity of reporter gene expression.

Determination of minimum inhibitory concentration

Antimicrobial activities were determined by MIC, which is defined as the lowest concentration of antimicrobial agents without visible growth. The antimicrobial susceptibility test was conducted using the broth microdilution assay in cation-adjusted Mueller-Hinton broth (Oxoid) for MRSA and VRSA, and in LB broth (BD Difco) for *B. subtilis* according to the CLSI guideline (46). Vancomycin, oxacillin, and CUHK242 were diluted from 256 to 0.25 µg/mL. Gentamicin, ciprofloxacin, and kanamycin were diluted from 64 to 0.0625 µg/mL. Rifampicin was diluted from 2 to 0.00195 µg/mL, as its MICs against *S. aureus* strains were typically ~0.0078 µg/mL. Each bacterial inoculum was adjusted to ~5 × 10^5 CFU/mL. Results were read after incubation at 37°C for 20 h. Experiments were performed in duplicates.

Growth curve of BS168 and BS2019

BS2019 and BS168 were streaked on LB agar plates and incubated at 37 °C overnight. The colonies were inoculated into LB broth to make a starting culture with OD_{600} ~0.1. The culture was incubated at 37 °C with OD_{600} measured at the first 10 min and every 15 min thereafter. The growth curve was plotted and analyzed using GraphPad Prism.

Time-kill kinetics assay

Time-kill kinetics assay adapted from the guidelines of CLSI was performed (71, 72). BS2019 or MRSA USA300 strain JE2 LAC was streaked on an LB agar plate and incubated overnight. The colonies were inoculated into LB or tryptic soy broth (TSB) to prepare the starter culture at OD_{600} ~0.1. The culture was incubated at 37 °C with shaking until OD_{600} ~0.2. Bacterial cells at log phase were suspended at ~1.5 × 10^6 CFU/mL in fresh media containing rifampicin, or chloramphenicol, or ampicillin, or CUHK242 at various concentrations along with untreated controls. For BS2019, samples were collected upon the single end point at 5 min post administration. For MRSA USA300, samples were collected at 0, 2, and 4 h in triplicates, followed by 10-fold serial dilutions in sterile phosphate-buffered saline (PBS). Five microliters of samples were spotted on Colombia agar plates supplemented with 5% defibrinated horse blood and incubated at 37 °C overnight. The visible colonies were counted and expressed as CFU/mL. The figures were plotted using GraphPad Prism.

Resistance generation by serial passage

Fresh colonies of *S. aureus* ATCC 29213 and MRSA USA300 strain JE2 LAC were obtained by streaking from glycerol stock onto LB agar and incubated overnight at 37 °C. On Day 0, colonies were resuspended in MHB and used to inoculate a broth microdilution plate set up to determine the MICs of CUHK242 and rifampicin in triplicates according to CLSI guidelines on determining antimicrobial susceptibility. From Day 1 onward, the latest MIC values of CUHK242 and rifampicin were recorded upon each passage, and the wells containing cells cultured under ¼ × MIC of both antimicrobial in each replicate lane were homogenized and used to prepare inocula for their corresponding fresh replicate lanes. Throughout the assay, each plate was covered with sterile breathable seals to prevent evaporation and incubated overnight at 37 °C with constant agitation at 340 rpm on a 3-mm orbital plate shaker. This process was repeated until its conclusion on Day 15.

Cell-based reporter assay

All the strains constructed and used in this study are listed in Table 1. Strains were streaked onto LB agar supplemented with 15 µg/mL spectinomycin and incubated at 37 °C overnight. A single colony was then picked and inoculated into LB broth supplemented with 15 µg/mL spectinomycin, followed by incubation at 37 °C with shaking overnight. The overnight culture was diluted with fresh LB to achieve OD_{600} ~0.05 and incubated at 37 °C with shaking until attaining an OD_{600} of 0.4. The culture was then divided into an drug-free untreated control group and a drug-treated group. Following the addition of antimicrobial compounds, 1% xylose was added into both groups to induce transcription of reporter gene. Starting from $T = 0$ at 1 min intervals, transcription reaction was arrested by transferring 1 mL aliquots of each cell culture into pre-cooled 0.4 mL stop buffer (60% ethanol, 2% phenol, 10 mM EDTA) for RT-qPCR sample preparation and analysis. Samples without exposure to stop buffer were collected for pellet harvesting for NanoLuc enzymatic assay. Control groups without treatment by antimicrobial agents were also included. The mixture was centrifuged at 5,000 × *g* at 4 °C for 5 min to harvest cell pellets, which were then stored at −80 °C until further use.

Quantification of transcription level by RT-qPCR analysis

Cell pellets were lyzed by glass beads, and total RNA was extracted using the Monarch Total RNA Miniprep Kit (NEB) following the manufacturer's instructions. Purified RNA was then used for template preparation with the High-Capacity cDNA Reverse Transcription Kit (Applied Biosystems). cDNA concentration was measured by Qubit ssDNA Assay Kit (Invitrogen) using Qubit 4 Fluorometer and diluted into working concentrations of 2.5 ng/µL. Twenty microliters of qPCR reaction mixtures each containing 10 µL PowerUp SYBR Green Master Mix (Applied Biosystems), 2 µL 5 µM forward primer, 2 µL 5 µM reverse primer, 2 µL cDNA, and 4 µL dH_2O was prepared, and qPCR was performed by QuantStudio 3 Real-time PCR System (Thermo Fisher). The abundance of target gene was presented as $2^{-\Delta C_T}$. The data were calculated relative to time $T = 0$, presented as $2^{C_T0 - C_Ti}$ ($C_T0 \geq C_Ti$) or $-2^{C_Ti - C_T0}$ ($C_T0 < C_Ti$). Mean values and standard deviation were calculated. Primers used for qPCR were listed in Table S1.

Quantification of translation level by NanoLuc enzymatic assay

Continuing from Section 5.6, cell pellets without exposure to transcription stop buffer were resuspended and incubated with lysis buffer containing B-PER Complete Bacterial Protein Extraction Reagent (Thermo Fisher) diluted in PBS in a 1:1 vol ratio, supplemented with a 0.01% protease inhibitor cocktail (P8849, Sigma) at room temperature for 30 min. Twenty-five microliters of cell lysates were added into a white 96-well plate in triplicates, followed by adding 25 µL Nano-Glo Luciferase Assay substrate (Promega) diluted 1:100 with assay buffer into a working solution. The luminescence was measured with a BioTek Synergy H1 (Agilent Technologies) multiplate reader. The raw data were taken in physical units (counts per second) and normalized against readings of the control groups at $T = 0$. The mean values and standard deviations were calculated using Microsoft Excel and plotted in GraphPad Prism.

Purification of RNAP CH and σ with NanoLuc fragment tags

E. coli BL21 (DE3) cells transformed with the overproduction plasmids were grown in 800 mL of autoinduction media supplemented with 0.5% (vol/vol) glycerol and 100 µg/mL ampicillin for selection at room temperature for 48 h. Cells were harvested at 5,000 × *g* for 5 min. The resulting pellet was lysed in 5 mL/gram lysis buffer (20 mM NaH_2PO_4, 500 mM NaCl, 20 mM imidazole, pH 8.0) diluted in with B-PER Complete Bacterial Protein Extraction Reagent (Thermo Fisher) at a 1:1 vol ratio. Following sonication and clarification at 8,000 × *g* for 1 h, the filtered supernatant passed through

a 1 mL His-trap FF column (Cytiva) pre-equilibrated with the lysis buffer without B-PER Complete Bacterial Protein Extraction Reagent (Thermo Fisher). Non-specific binding was removed by 10 CV of wash buffer (20 mM NaH_2PO_4, 500 mM NaCl, 40 mM imidazole, pH 8.0), and the his-tagged proteins were eluted by elution buffer (20 mM NaH_2PO_4, 500 mM NaCl, 500 mM imidazole, pH 8.0). Fractions consisting of the target proteins were pooled and dialyzed into PBS with 30% glycerol before storage at −80 °C.

In vitro NanoLuc PPI inhibition assay

A formerly established split luciferase-based PPI inhibition assay was adapted (27). Compound CUHK242 was dissolved to 10 mg/mL in DMSO. Twofold dilution of CUHK242 was performed in PBS, starting from 3 mM. Forty microliters of C-LgBiT-σ (2.5 µM in PBS) was added to 96-well plates and then mixed with 20 µL of CUHK242 at varying concentrations for 10 min at 37 °C. Forty microliters of C-SmBiT-CH (2.5 µM in PBS) was added, and the reaction was incubated for 10 min at 37 °C, followed by the addition of 20 µL of Promega Nano-Glo Luciferase Assay Substrate (Promega). Luminescence signals were measured using a BioTek Synergy H1 plate reader. The experiment was performed in triplicate. Technical repeats were taken for data reproducibility.

Data and statistical analysis

For biochemical assays, technical repeats were performed to ensure reproducibility. Two-way ANOVA was used to measure the statistical significance, presented in GraphPad Prism style: $P \leq 0.05$ (*), ≤ 0.01 (**), ≤ 0.001 (***), ≤ 0.0001 (****).

Rabbit red blood cell lysis assay

A major hallmark of virulence in pathogenic *S. aureus* strains is the production of the secretory exotoxin α-toxin (α-hemolysin) (73–75). The hemolysis of rabbit erythrocytes by purified staphylococcal α-toxin is a well-established methodology characterized by enzyme-like sigmoidal response curves directly proportional to toxin concentrations and had since been optimized and employed in our previous work on other novel antimicrobial candidates (72, 76). To investigate the effect of antimicrobial agent treatment on α-toxin production, ¼ × MIC of each test compound was added to liquid cultures of MRSA USA300 strain JE2 LAC grown to early exponential phase in TSB. Following overnight incubation at 37 °C and agitated at 175 rpm, the now post-stationary phase cultures were harvested by centrifugation at 8,000 × *g* for 3 min and the supernatants collected. Rabbit RBCs were packed by washing gently in sterile PBS until no hemolysis was observed, whereupon cells were resuspended as a 3% solution in PBS. Harvested sample supernatants were twofold serially diluted and incubated with 3% RBC suspension in a 1:10 ratio (i.e., 20 µL supernatant to 180 µL RBC suspension per well) in a 48-well microplate for 1 h at 37 °C. A PBS-only negative control was included alongside a positive control group using 1% Triton X-100. The amount of hemoglobin released was determined by measuring the absorbance at 540 nm, and % cell lysis was calculated as sample absorbance/positive control absorbance.

ACKNOWLEDGMENTS

The research was supported by the Research Grants Council of Hong Kong (14107919 to X.Y., C5008-19G and 15100021 to C.M.), Hong Kong Food and Health Bureau (HMRF 19180052 to X.Y.), the Chinese University of Hong Kong (Faculty of Medicine Faculty Innovation Award FIA2018/A/03, Passion for Perfection Scheme PFP202210-008 to X.Y.), and the Hong Kong Polytechnic University (1-ZE2E and State Key Laboratory of Chemical Biology and Drug Discovery to C.M.).

The authors would like to thank Ms. Lin Lin for her technical assistance in performing NanoLuc assays.

X.Y. and C.M. conceived the idea. N.M.L., X.Y., T.F.T., J.Q., M.W.T., Y.T., C.H.K., Q.Z., and K.H.C. performed the experiments. N.M.L., X.Y., T.F.T., A.J.C. and C.M. analyzed the data and wrote the paper.

AUTHOR AFFILIATIONS

[1]Department of Microbiology, The Chinese University of Hong Kong, Prince of Wales Hospital, Hong Kong Special Administrative Region, China
[2]State Key Laboratory of Chemical Biology and Drug Discovery, Department of Applied Biology and Chemical Technology, The Hong Kong Polytechnic University, Hong Kong Special Administrative Region, China

AUTHOR ORCIDs

Nga Man Lam http://orcid.org/0000-0003-1400-6211
Tsz Fung Tsang http://orcid.org/0000-0001-7904-277X
Jiayi Qu http://orcid.org/0009-0001-8790-6571
Man Wai Tsang http://orcid.org/0009-0001-3206-5779
Yuan Tao http://orcid.org/0009-0006-1869-0777
Cheuk Hei Kan http://orcid.org/0000-0003-1246-4809
Qingyu Zou http://orcid.org/0009-0007-6712-8921
King Hong Chan http://orcid.org/0000-0001-7908-4857
Adrian Jun Chu http://orcid.org/0000-0001-9206-9395
Cong Ma http://orcid.org/0000-0001-9245-0356
Xiao Yang http://orcid.org/0000-0002-3071-6531

FUNDING

Funder	Grant(s)	Author(s)
Hong Kong Research Grants Council	14107919	Xiao Yang
Hong Kong Research Grants Council	C5008-19G, 15100021	Cong Ma
Hong Kong Food and Bureau	HMRF 19180052	Xiao Yang
Chinese University of Hong Kong (CUHK)	FIA2018/A/03, PFP202210-008	Xiao Yang
Hong Kong Polytechnic University (PolyU)	1-ZE2E	Cong Ma

ADDITIONAL FILES

The following material is available online.

Supplemental Material

Supplemental material (AEM00717-S0001.docx). Tables S1 and S2; Figures S1 and S2.
Graphical abstract (AEM00717-24-S0002.tif). Diagrammatic summary of the study.

REFERENCES

1. Murray CJL, Ikuta KS, Sharara F, Swetschinski L, Robles Aguilar G, Gray A, Han C, Bisignano C, Rao P, Wool E, et al. 2022. Global burden of bacterial antimicrobial resistance in 2019: a systematic analysis. The Lancet 399:629–655. https://doi.org/10.1016/S0140-6736(21)02724-0
2. Appelbaum PC. 2006. The emergence of vancomycin-intermediate and vancomycin-resistant *Staphylococcus aureus*. Clin Microbiol Infect 12 Suppl 1:16–23. https://doi.org/10.1111/j.1469-0691.2006.01344.x
3. Ho PL, Lo PY, Chow KH, Lau EHY, Lai EL, Cheng VCC, Kao RY. 2010. Vancomycin MIC creep in MRSA isolates from 1997 to 2008 in a healthcare region in Hong Kong. J Infect 60:140–145. https://doi.org/10.1016/j.jinf.2009.11.011
4. Steinkraus G, White R, Friedrich L. 2007. Vancomycin MIC creep in non-vancomycin-intermediate *Staphylococcus aureus* (VISA), vancomycin-susceptible clinical methicillin-resistant *S-aureus* (MRSA) blood isolates from 2001-05. J Antimicrob Chemother 60:788–794. https://doi.org/10.1093/jac/dkm258
5. Brown NM, Goodman AL, Horner C, Jenkins A, Brown EM. 2021. Treatment of methicillin-resistant *Staphylococcus aureus* (MRSA): updated guidelines from the UK. JAC-Antimicrobial Resistance 3. https://doi.org/10.1093/jacamr/dlaa114
6. Ma C, Yang X, Lewis PJ. 2016. Bacterial transcription as a target for antibacterial drug development. Microbiol Mol Biol Rev 80:139–160. https://doi.org/10.1128/MMBR.00055-15
7. Kavčič B, Tkačik G, Bollenbach T. 2020. Mechanisms of drug interactions between translation-inhibiting antibiotics. Nat Commun 11:4013. https://doi.org/10.1038/s41467-020-17734-z

8. Ude S, Lassak J, Starosta AL, Kraxenberger T, Wilson DN, Jung K. 2013. Translation elongation factor EF-P alleviates ribosome stalling at polyproline stretches. Science 339:82–85. https://doi.org/10.1126/science.1228985
9. Studer SM, Joseph S. 2006. Unfolding of mRNA secondary structure by the bacterial translation initiation complex. Mol Cell 22:105–115. https://doi.org/10.1016/j.molcel.2006.02.014
10. Haldenwang WG. 1995. The sigma factors of *Bacillus subtilis*. Microbiol Rev 59:1–30. https://doi.org/10.1128/mr.59.1.1-30.1995
11. Browning DF, Busby SJW. 2016. Local and global regulation of transcription initiation in bacteria. Nat Rev Microbiol 14:638–650. https://doi.org/10.1038/nrmicro.2016.103
12. Yang X, Luo MJ, Yeung ACM, Lewis PJ, Chan PKS, Ip M, Ma C. 2017. First-in-class inhibitor of ribosomal RNA synthesis with antimicrobial activity against *Staphylococcus aureus*. Biochemistry 56:5049–5052. https://doi.org/10.1021/acs.biochem.7b00349
13. Ye JQ, Chu AJ, Lin L, Chan ST, Harper R, Xiao M, Artsimovitch I, Zuo Z, Ma C, Yang X. 2020. Benzyl and benzoyl benzoic acid inhibitors of bacterial RNA polymerase-sigma factor interaction. European Journal of Medicinal Chemistry 208:112671. https://doi.org/10.1016/j.ejmech.2020.112671
14. Artsimovitch I, Seddon J, Sears P. 2012. Fidaxomicin is an inhibitor of the initiation of bacterial RNA synthesis. Clin Infect Dis 55 Suppl 2:S127–31. https://doi.org/10.1093/cid/cis358
15. Wilson DN. 2009. The A-Z of bacterial translation inhibitors. Crit Rev Biochem Mol Biol 44:393–433. https://doi.org/10.3109/-10409230903307311
16. Boyle WK, Hall LS, Armstrong AA, Dulebohn DP, Samuels DS, Gherardini FC, Bourret TJ. 2020. Establishment of an *in vitro* RNA polymerase transcription system: a new tool to study transcriptional activation in *Borrelia burgdorferi*. Sci Rep 10:8246. https://doi.org/10.1038/s41598-020-65104-y
17. Berger M, Aijaz I, Berger P, Dobrindt U, Koudelka G. 2019. Transcriptional and translational inhibitors block SOS response and shiga toxin expression in enterohemorrhagic *Escherichia coli*. Sci Rep 9. https://doi.org/10.1038/s41598-019-55332-2
18. Davies KM, Lewis PJ. 2003. Localization of rRNA synthesis in *Bacillus subtilis*: characterization of loci involved in transcription focus formation. J Bacteriol 185:2346–2353. https://doi.org/10.1128/JB.185.7.2346-2353.2003
19. Ma C, Yang X, Lewis PJ. 2016. Bacterial transcription inhibitor of RNA polymerase holoenzyme formation by structure-based drug design: from *in Silico* screening to validation. ACS Infect. Dis 2:39–46. https://doi.org/10.1021/acsinfecdis.5b00058
20. Ulijasz AT, Grenader A, Weisblum B. 1996. A vancomycin-inducible lacZ reporter system in *Bacillus subtilis*: induction by antibiotics that inhibit cell wall synthesis and by lysozyme. J Bacteriol 178:6305–6309. https://doi.org/10.1128/jb.178.21.6305-6309.1996
21. Zaslaver A, Bren A, Ronen M, Itzkovitz S, Kikoin I, Shavit S, Liebermeister W, Surette MG, Alon U. 2006. A comprehensive library of fluorescent transcriptional reporters for *Escherichia coli*. Nat Methods 3:623–628. https://doi.org/10.1038/nmeth895
22. Cao M, Wang T, Ye R, Helmann JD. 2002. Antibiotics that inhibit cell wall biosynthesis induce expression of the *Bacillus subtilis* sigma(W) and sigma(M) regulons. Mol Microbiol 45:1267–1276. https://doi.org/10.1046/j.1365-2958.2002.03050.x
23. Hirano M, Ando R, Shimozono S, Sugiyama M, Takeda N, Kurokawa H, Deguchi R, Endo K, Haga K, Takai-Todaka R, Inaura S, Matsumura Y, Hama H, Okada Y, Fujiwara T, Morimoto T, Katayama K, Miyawaki A. 2022. A highly photostable and bright green fluorescent protein. Nat Biotechnol 40:1132–1142. https://doi.org/10.1038/s41587-022-01278-2
24. Heppert JK, Dickinson DJ, Pani AM, Higgins CD, Steward A, Ahringer J, Kuhn JR, Goldstein B. 2016. Comparative assessment of fluorescent proteins for *in vivo* imaging in an animal model system. MBoC 27:3385–3394. https://doi.org/10.1091/mbc.e16-01-0063
25. England CG, Ehlerding EB, Cai WB. 2016. NanoLuc: a small Luciferase is brightening up the field of bioluminescence. Bioconjug Chem 27:1175–1187. https://doi.org/10.1021/acs.bioconjchem.6b00112
26. Dixon AS, Schwinn MK, Hall MP, Zimmerman K, Otto P, Lubben TH, Butler BL, Binkowski BF, Machleidt T, Kirkland TA, Wood MG, Eggers CT, Encell LP, Wood KV. 2016. NanoLuc complementation reporter optimized for accurate measurement of protein interactions in cells. ACS Chem Biol 11:400–408. https://doi.org/10.1021/acschembio.5b00753
27. Tsang TF, Qiu YY, Lin L, Ye JQ, Ma C, Yang X. 2019. Simple method for studying *in vitro* protein-protein interactions based on protein complementation and its application in drug screening targeting bacterial transcription. ACS Infect Dis 5:521–527. https://doi.org/10.1021/acsinfecdis.9b00020
28. Stacer AC, Nyati S, Moudgil P, Iyengar R, Luker KE, Rehemtulla A, Luker GD. 2013. Nanoluc reporter for dual Luciferase imaging in living animals. Mol Imaging 12:1–13. https://doi.org/10.2310/7290.2013.00062
29. Su Y, Walker JR, Park Y, Smith TP, Liu LX, Hall MP, Labanieh L, Hurst R, Wang DC, Encell LP, Kim N, Zhang F, Kay MA, Casey KM, Majzner RG, Cochran JR, Mackall CL, Kirkland TA, Lin MZ. 2020. Novel NanoLuc substrates enable bright two-population bioluminescence imaging in animals. Nat Methods 17:852–860. https://doi.org/10.1038/s41592-020-0889-6
30. Hutter B, Fischer C, Jacobi A, Schaab C, Loferer H. 2004. Panel of *Bacillus subtilis* reporter strains indicative of various modes of action. Antimicrob Agents Chemother 48:2588–2594. https://doi.org/10.1128/AAC.48.7.2588-2594.2004
31. Waidmann MS, Bleichrodt FS, Laslo T, Riedel CU. 2011. Bacterial luciferase reporters: the Swiss army knife of molecular biology. Bioeng Bugs 2:8–16. https://doi.org/10.4161/bbug.2.1.13566
32. Loh JMS, Proft T. 2014. Comparison of firefly luciferase and NanoLuc luciferase for biophotonic labeling of group A Streptococcus. Biotechnol Lett 36:829–834. https://doi.org/10.1007/s10529-013-1423-z
33. Proshkin S, Rahmouni AR, Mironov A, Nudler E. 2010. Cooperation between translating ribosomes and RNA polymerase in transcription elongation. Science 328:504–508. https://doi.org/10.1126/science.1184939
34. Zhu ML, Mori M, Hwa T, Dai XF. 2019. Disruption of transcription-translation coordination in *Escherichia coli* leads to premature transcriptional termination. Nat Microbiol 4:2347–2356. https://doi.org/10.1038/s41564-019-0543-1
35. Rafailidis PI, Ioannidou EN, Falagas ME. 2007. Ampicillin/Sulbactam - current status in severe bacterial infections. Drugs 67:1829–1849. https://doi.org/10.2165/00003495-200767130-00003
36. Zapun A, Contreras-Martel C, Vernet T. 2008. Penicillin-binding proteins and beta-lactam resistance. FEMS Microbiol Rev 32:361–385. https://doi.org/10.1111/j.1574-6976.2007.00095.x
37. Ye JQ, Chu AJ, Harper R, Chan ST, Shek TL, Zhang YF, Ip M, Sambir M, Artsimovitch I, Zuo Z, Yang X, Ma C. 2020. Discovery of antibacterials that inhibit bacterial RNA polymerase interactions with sigma factors. J. Med. Chem. 63:7695–7720. https://doi.org/10.1021/acs.jmedchem.0c00520
38. Lewis PJ, Marston AL. 1999. GFP vectors for controlled expression and dual labelling of protein fusions in *Bacillus subtilis*. Gene 227:101–110. https://doi.org/10.1016/s0378-1119(98)00580-0
39. Hiblot J, Yu QLY, Sabbadini MDB, Reymond L, Xue L, Schena A, Sallin O, Hill N, Griss R, Johnsson K. 2017. Luciferases with tunable emission wavelengths. Angew Chem Int Ed Engl 56:14556–14560. https://doi.org/10.1002/anie.201708277
40. Klumpp S, Zhang Z, Hwa T. 2009. Growth rate-dependent global effects on gene expression in bacteria. Cell 139:1366–1375. https://doi.org/10.1016/j.cell.2009.12.001
41. Zumla A, Nahid P, Cole ST. 2013. Advances in the development of new tuberculosis drugs and treatment regimens. Nat Rev Drug Discov 12:388–404. https://doi.org/10.1038/nrd4001
42. Tiberi S, Plessis N, Walzl G, Vjecha MJ, Rao M, Ntoumi F, Mfinanga S, Kapata N, Mwaba P, McHugh TD, Ippolito G, Migliori GB, Maeurer MJ, Zumla A. 2018. Tuberculosis: progress and advances in development of new drugs, treatment regimens, and host-directed therapies. Lancet infect DIS 18:e183–e198. https://doi.org/10.1016/S1473--3099(18)30110-5
43. Drago L. 2019. Chloramphenicol resurrected: a journey from antibiotic resistance in eye infections to biofilm and ocular microbiota. Microorganisms 7:278. https://doi.org/10.3390/microorganisms7090278
44. Fukuda M, Ohashi H, Matsumoto C, Mishima S, Shimomura Y. 2002. Methicillin-resistant *Staphylococcus aureus* and methicillin-resistant coagulase-negative Staphylococcus ocular surface infection efficacy of

chloramphenicol eye drops. Cornea 21:S86–9. https://doi.org/10.1097/01.ico.0000263125.99262.42
45. Lam TP, Ho PL, Lam KF, Choi K, Yung R. 2009. Use of antibiotics by primary care doctors in Hong Kong. Asia Pac Fam Med 8:5. https://doi.org/10.1186/1447-056X-8-5
46. CLSI. 2020. Performance standards for antimicrobial susceptibility testing. Clinical and Laboratory Standards Institute, Wayne, PA.
47. Shaw KJ, Miller N, Liu XJ, Lerner D, Wan J, Bittner A, Morrow BJ. 2003. Comparison of the changes in global gene expression of *Escherichia coli* induced by four bactericidal agents. J Mol Microbiol Biotechnol 5:105–122. https://doi.org/10.1159/000069981
48. Chen CJ, Huang YC. 2014. New epidemiology of *Staphylococcus aureus* infection in Asia. Clin Microbiol Infect 20:605–623. https://doi.org/10.1111/1469-0691.12705
49. Mediavilla JR, Chen L, Mathema B, Kreiswirth BN. 2012. Global epidemiology of community-associated methicillin resistant *Staphylococcus aureus* (CA-MRSA). Current Opinion in Microbiology 15:588–595. https://doi.org/10.1016/j.mib.2012.08.003
50. Monecke S, Coombs G, Shore AC, Coleman DC, Akpaka P, Borg M, Chow H, Ip M, Jatzwauk L, Jonas D, Kadlec K, Kearns A, Laurent F, O'Brien FG, Pearson J, Ruppelt A, Schwarz S, Scicluna E, Slickers P, Tan H-L, Weber S, Ehricht R. 2011. A field guide to pandemic, epidemic and sporadic clones of methicillin-resistant *Staphylococcus aureus*. PLoS One 6:e17936. https://doi.org/10.1371/journal.pone.0017936
51. Kaatz GW, Seo SM, Ruble CA. 1991. Mechanisms of fluoroquinolone resistance in *Staphylococcus-aureus*. J Infect Dis 163:1080–1086. https://doi.org/10.1093/infdis/163.5.1080
52. Ross JI, Eady EA, Cove JH, Baumberg S. 1996. Minimal functional system required for expression of erythromycin resistance by msrA in *Staphylococcus aureus* RN4220. Gene 183:143–148. https://doi.org/10.1016/s0378-1119(96)00541-0
53. Chan BCL, Ip M, Gong H, Lui SL, See RH, Jolivalt C, Fung KP, Leung PC, Reiner NE, Lau CBS. 2013. Synergistic effects of diosmetin with erythromycin against ABC transporter over-expressed methicillin-resistant *Staphylococcus aureus* (MRSA) RN4220/pUL5054 and inhibition of MRSA pyruvate kinase. Phytomedicine 20:611–614. https://doi.org/10.1016/j.phymed.2013.02.007
54. Ho PL, Chow KH, Lo PY, Lee KF, Lai EL. 2009. Changes in the epidemiology of methicillin-resistant *Staphylococcus aureus* associated with spread of the ST45 lineage in Hong Kong (DMID-08-518 revised). Diagn Microbiol Infect Dis 64:131–137. https://doi.org/10.1016/j.diagmicrobio.2009.01.030
55. Tenover FC, McAllister S, Fosheim G, McDougal LK, Carey RB, Limbago B, Lonsway D, Patel JB, Kuehnert MJ, Gorwitz R. 2008. Characterization of *Staphylococcus aureus* isolates from nasal cultures collected from individuals in the United States in 2001 to 2004. J Clin Microbiol 46:2837–2841. https://doi.org/10.1128/JCM.00480-08
56. Gorwitz RJ, Kruszon-Moran D, McAllister SK, McQuillan G, McDougal LK, Fosheim GE, Jensen BJ, Killgore G, Tenover FC, Kuehnert MJ. 2008. Changes in the prevalence of nasal colonization with *Staphylococcus aureus* in the United States, 2001-2004. J Infect Dis 197:1226–1234. https://doi.org/10.1086/533494
57. Yang J, Barra JT, Fung DK, Wang JD. 2022. *Bacillus subtilis* produces (p)ppGpp in response to the bacteriostatic antibiotic chloramphenicol to prevent its potential bactericidal effect. mLife 1:101–113. https://doi.org/10.1002/mlf2.12031
58. Bass IA, Danilevskaya ON, Mekhedov SL, Fedoseeva VB, Gorlenko ZM. 1979. Effect of rifampicin upon the transcription of RNA-polymerase beta-gene in *Escherichia-coli*. Molec Gen Genet 173:101–107. https://doi.org/10.1007/BF00267695
59. Bandow JE, Brötz H, Hecker M. 2002. *Bacillus subtilis* tolerance of moderate concentrations of rifampin involves the sigma(B)-dependent general and multiple stress response. J Bacteriol 184:459–467. https://doi.org/10.1128/JB.184.2.459-467.2002
60. Fukuda R, Nagasawa-Fujimori H. 1983. Mechanism of the rifampicin induction of RNA polymerase beta and beta' subunit synthesis in *Escherichia coli*. J Biol Chem 258:2720–2728.
61. Rojas-Tapias DF, Helmann JD. 2018. Induction of the Spx regulon by cell wall stress reveals novel regulatory mechanisms in *Bacillus subtilis*. Mol Microbiol 107:659–674. https://doi.org/10.1111/mmi.13906
62. Campbell EA, Korzheva N, Mustaev A, Murakami K, Nair S, Goldfarb A, Darst SA. 2001. Structural mechanism for rifampicin inhibition of bacterial RNA polymerase. Cell 104:901–912. https://doi.org/10.1016/s0092-8674(01)00286-0
63. Syroegin EA, Flemmich L, Klepacki D, Vazquez-Laslop N, Micura R, Polikanov YS. 2022. Structural basis for the context-specific action of the classic peptidyl transferase inhibitor chloramphenicol. Nat Struct Mol Biol 29:152–161. https://doi.org/10.1038/s41594-022-00720-y
64. Svetlov MS, Plessa E, Chen CW, Bougas A, Krokidis MG, Dinos GP, Polikanov YS. 2019. High-resolution crystal structures of ribosome-bound chloramphenicol and erythromycin provide the ultimate basis for their competition. RNA 25:600–606. https://doi.org/10.1261/rna.069260.118
65. Qiu Y, Chu AJ, Tsang TF, Zheng Y, Lam NM, Li KSL, Ip M, Yang X, Ma C. 2022. Synthesis and biological evaluation of nusbiarylin derivatives as bacterial rRNA synthesis inhibitor with potent antimicrobial activity against MRSA and VRSA. Bioorg Chem 124:105863. https://doi.org/10.1016/j.bioorg.2022.105863
66. Ye J, Kan CH, Zheng Y, Tsang TF, Chu AJ, Chan KH, Yang X, Ma C. 2024. Sulfonamidyl derivatives of sigmacidin: protein-protein interaction inhibitors targeting bacterial RNA polymerase and Sigma factor interaction exhibiting antimicrobial activity against antibiotic-resistant bacteria. Bioorg Chem 143:106983. https://doi.org/10.1016/j.bioorg.2023.106983
67. Brennan MA, Rosenthal AZ. 2021. Single-cell RNA sequencing elucidates the structure and organization of microbial communities. Front. Microbiol 12. https://doi.org/10.3389/fmicb.2021.713128
68. Callaghan JD, Stella NA, Lehner KM, Treat BR, Brothers KM, St Leger AJ, Shanks RMQ. 2020. Xylose-inducible promoter tools for *Pseudomonas* species and their use in Implicating a role for the type II secretion system protein XcpQ in the inhibition of corneal epithelial wound closure. Appl Environ Microbiol 86:e00250-20. https://doi.org/10.1128/AEM.00250-20
69. Petersohn A, Brigulla M, Haas S, Hoheisel JD, Völker U, Hecker M. 2001. Global analysis of the general stress response of *Bacillus subtilis*. J Bacteriol 183:5617–5631. https://doi.org/10.1128/JB.183.19.5617-5631.2001
70. Guldimann C, Boor KJ, Wiedmann M, Guariglia-Oropeza V. 2016. Resilience in the face of uncertainty: sigma factor B fine-tunes gene expression to support homeostasis in Gram-positive bacteria. Appl Environ Microbiol 82:4456–4469. https://doi.org/10.1128/AEM.00714-16
71. 1999. Methods for determining bactericidal activity of antimicrobial agents. The Clinical and Laboratory Standards Institute, Wayne, PA.
72. Chu AJ, Qiu Y, Harper R, Lin L, Ma C, Yang X. 2020. Nusbiarylins inhibit transcription and target virulence factors in bacterial pathogen *Staphylococcus aureus* Int J Mol Sci 21:5772. https://doi.org/10.3390/ijms21165772
73. Tavares A, Nielsen JB, Boye K, Rohde S, Paulo AC, Westh H, Schønning K, de Lencastre H, Miragaia M. 2014. Insights into alpha-hemolysin (Hla) evolution and expression among *Staphylococcus aureus* clones with hospital and community origin. PLoS One 9:e98634. https://doi.org/10.1371/journal.pone.0098634
74. Kebaier C, Chamberland RR, Allen IC, Gao X, Broglie PM, Hall JD, Jania C, Doerschuk CM, Tilley SL, Duncan JA. 2012. Staphylococcus aureus alpha-hemolysin mediates virulence in a murine model of severe pneumonia through activation of the NLRP3 inflammasome. J Infect Dis 205:807–817. https://doi.org/10.1093/infdis/jir846
75. Cheung GYC, Bae JS, Otto M. 2021. Pathogenicity and virulence of *Staphylococcus aureus*. Virulence 12:547–569. https://doi.org/10.1080/21505594.2021.1878688
76. Madoff MA, Cooper LZ, Weinstein L. 1964. Hemolysis of rabbit erythrocytes by purified Staphylococcal alpha-toxin. I. J Bacteriol 87:145–149. https://doi.org/10.1128/jb.87.1.145-149.1964